

Towards Enhanced Analysis of Lung Cancer Lesions in EBUS-TBNA: A Semi-Supervised Video Object Detection Method

Ching-Kai Lin^{1,2,3,4}, Jyun-An Lin^{4*}, Yun-Chien Cheng^{4*},

¹ Department of Medicine, National Taiwan University Cancer Center, Taipei, Taiwan

² Department of Internal Medicine, National Taiwan University Hospital, Taipei, Taiwan

³ Department of Internal Medicine, National Taiwan University Hsin-Chu Hospital, Hsin-Chu, Taiwan

⁴ Department of Mechanical Engineering, College of Engineering, National Yang Ming Chiao Tung University, Hsin-Chu, Taiwan

*Corresponding author: yccheng@nycu.edu.tw, andy.en11@nycu.edu.tw

Abstract

This study aims to establish a computer-aided diagnostic system for lung lesions using bronchoscope endobronchial ultrasound (EBUS) to assist physicians in identifying lesion areas. During EBUS-transbronchial needle aspiration (EBUS-TBNA) procedures, physicians rely on grayscale ultrasound images to determine the location of lesions. However, these images often contain significant noise and can be influenced by surrounding tissues or blood vessels, making interpretation challenging. Previous research has lacked the application of object detection models to EBUS-TBNA, and there has been no well-defined solution for annotating the EBUS-TBNA dataset. In related studies on ultrasound images, although models have been successful in capturing target regions for their respective tasks, their training and predictions have been based on two-dimensional images, limiting their ability to leverage temporal features for improved predictions. This study introduces a three-dimensional image-based object detection model. It utilizes an attention mechanism to capture temporal correlations and we will implement a filtering mechanism to select relevant information from previous frames. Subsequently, a teacher-student model training approach is employed to optimize the model further, leveraging unlabeled data. To mitigate the impact of poor-quality pseudo-labels on the student model, we will add a special Gaussian Mixture Model (GMM) to ensure the quality of pseudo-labels. To align with the characteristics of the EBUS-TBNA dataset, optical flow is introduced to automatically generate additional labels from manually annotated data, enhancing the model's performance. Test results demonstrate that this model, employing spatiotemporal information capture, achieves a mean Average Precision (mAP) of 41.9 on the test dataset, outperforming other models. This study also confirmed that the semi-supervised learning method can improve the performance of the model compared with the traditional optical flow method in generating pseudo labels in EBUS-TBNA.

Keywords: Deep learning, Lung cancer, Vision Transformer, Endobronchial ultrasound-guided transbronchial needle aspiration, Mediastinal lesions, Video object detection

1. Introduction

Lung cancer is the leading cause of cancer incidence and mortality [1], and early diagnosis with accurate staging is crucial for subsequent treatment planning [2]. In the diagnostic process, live biopsy surgeries are commonly employed. Endobronchial ultrasound-guided transbronchial needle aspiration (EBUS-TBNA) is a

relatively new minimally invasive technique widely used for sampling lesions in the mediastinal cavity and lung hilum. Previous studies have confirmed its high accuracy in diagnosing and staging malignant lung tumors [3-6]. Within the limited anesthesia time, being able to accurately locate and sample lesions on ultrasound videos can effectively improve the efficiency and accuracy of physicians during surgery, thereby reducing the risks associated with the procedure.

EBUS-TBNA imaging includes three modalities: grayscale, Doppler, and elastography. Grayscale is used to locate lesions and perform initial analysis of lesion features [7]. Doppler detects blood flow signals around lymph nodes, confirming the condition of lymph nodes and other tissues [8]. Elastography measures the rigidity of mediastinal and hilar lymph nodes to further confirm whether they are malignant lesions [9]. Grayscale imaging is a prerequisite for subsequent imaging analysis. Although grayscale imaging can reveal the location of lesions, it is sometimes affected by interference such as blood vessels and noise. Bronchoscopic physicians also require more learning experience to familiarize themselves with these imaging features. Therefore, efficiently analyzing the features of grayscale imaging to quickly identify suitable lesions for subsequent benign-malignant interpretation is essential.

To implement an automated diagnostic system, previous studies utilized object detection models from deep learning on ultrasound images [10-14] to generate prediction boxes. Among these models, the transformer architecture, particularly the design of DETR by the Tang et al [14], stands out. They employed this model to predict spinal curves and vertebral levels. In comparison with other research frameworks, DETR's unique attention mechanism is more effective in capturing global information to enhance performance. However, the methods used in the above-mentioned studies on ultrasound videos can only capture spatial information of the current frame and cannot obtain information in the temporal direction. During the surgical process, the location of the lesion changes over time, we believe that these two-dimensional structures are ineffective in capturing temporal information. This could lead to errors in recognizing dynamic EBUS-TBNA videos. Additionally, the annotation data in our dataset requires physicians to review the entire video to determine the lesion's location, making the acquisition of annotation data challenging. However, the mentioned methods do not address the handling of a small amount of annotated data.

To address the challenge of not capturing temporal information on dynamic EBUS-TBNA videos, we aim to design a video object detection model based on three-dimensional video data. A more recent approach is to modify DETR [15-17]. The objective is to leverage its

unique attention mechanism to obtain temporal relevance for acquiring time-related information. For example, the VSTAM architecture designed by the Masato et al [15] utilizes an attention ranking mechanism. It calculates attention between the decoder's output of the current frame and the results stored in external memory from previous frames. Those with high attention are stored in external memory. High-level feature maps are also calculated using an attention mechanism to learn the correlation between the current and previous frames, thus obtaining temporal information. And we aim to adapt such methods to design a video object detection model specifically for the EBUS-TBNA dataset. In EBUS-TBNA surgery, even slight movements of the probe result in significant changes in the lesion's position in ultrasound video. Therefore, we intend to utilize attention mechanisms to capture temporal information, incorporating a filtering mechanism to select regions with significant positional changes. This is to avoid interference from inappropriate temporal information in the prediction process.

Moreover, to address the issue of the labor cost associated with annotation data, we aim to efficiently utilize unlabeled data. Previous research has applied semi-supervised methods to object detection models [18-20], such as the consistent teacher design by the Zhang team [19]. In this approach, a pre-trained teacher generates pseudo-labels, and a GMM module with an adaptive assignment module filters out unsuitable portions. Finally, an FAM-3D module aligns the prediction boxes of the teacher and student models to enhance the accuracy of the student model. Existing semi-supervised learning studies mostly use a teacher-student model pair to improve the quality of pseudo-labels, increase the model's robustness, and thereby more effectively utilize unlabeled data. Among these, many of them employ GMM modules and methods for contrastive learning with added noise. The GMM module helps identify the distribution of target features. In EBUS-TBNA data, the predictions of the teacher model are more likely to be influenced by factors like blood vessels, tissues, etc., leading to potential misjudgments of lesion areas. Features that are prone to misjudgment are expected to deviate from the distribution of target features. Therefore, we aim to use the GMM module to filter out pseudo-labels that are less consistent with the lesion area, preventing the transmission of inaccurate information to the student model. Additionally, we intend to introduce contrastive learning with noise commonly found in EBUS-TBNA data, making the student model less susceptible to noise effects.

In the mentioned literature, it is evident that capturing temporal features in video data leads to stronger performance. Applying semi-supervised methods to object detection models effectively leverages unlabeled data for improved model performance.

However, there is currently no model well-suited for EBUS-TBNA data in the literature. Therefore, we aim to reference the aforementioned studies to design a semi-supervised object detection model based on video data.

While the application of object detection models in ultrasound images has validated the performance of deep learning architectures in analyzing EBUS-TBNA videos, we have identified the following challenges in existing techniques as follows:

- (1) No research has proposed effective methods to simultaneously acquire temporal information from ultrasound videos and integrate it with EBUS-TBNA videos.
- (2) Some model architectures proposed in previous studies do not address the difficulty in annotating data. Utilizing these models may result in degraded performance due to insufficient annotated data.

To enable the model to capture temporal information from dynamic EBUS-TBNA videos and apply it to clinical imaging, this study has improved and designed a three-dimensional model based on the Detection Transformer (DETR). In recent years, with the rise of transformer architectures, DETR has become a widely used deep learning framework for computer vision object detection tasks. Its powerful self-attention mechanism has demonstrated better accuracy than CNNs in various public datasets [21][22]. However, subsequent video object detection models derived from DETR, while exhibiting good performance, require large amounts of data for training due to their numerous parameters. This makes it challenging to apply DETR-based modified video object detection models to datasets with limited annotated data.

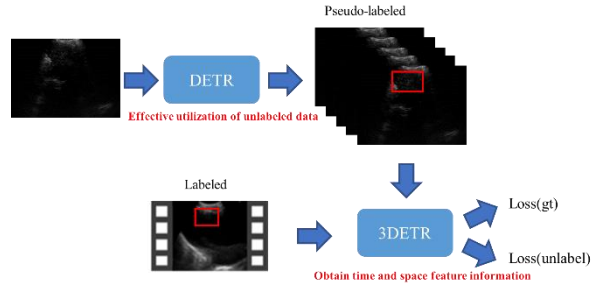


Figure 1. DEBUS effectively utilizes unlabeled data through a teacher-student model structure. Subsequently, it integrates the 3DETR to extract both temporal and spatial feature information from the videos.

To address this issue, we applied a semi-supervised learning approach to effectively utilize unlabeled data. Additionally, by observing EBUS-TBNA videos, we further tailored our approach to the characteristics of this data. The entire training framework is referred to as DEBUS, and its architectural features are illustrated in Figure 1.

The contributions of this study are summarized as follows:

- (1) This study aims to design a computer-assisted system capable of outlining lesions for reference by medical professionals.
- (2) The proposed 3DETR model in this study leverages the temporal sequence information in video to achieve higher performance.
- (3) The DEBUS framework is introduced, combining 3DETR with semi-supervised learning methods to reduce dependence on annotated datasets.
- (4) This study uses optical flow method and semi-supervised learning to generate EBUS-TBNA pseudo labels and examines the results of both.

In conclusion, the goal of this research is to develop a computer-assisted diagnostic system. Through the DEBUS framework, higher performance is achieved compared to existing methods, while also saving manpower and time costs in clinical applications. This system aims to provide real-time confidence scores and prediction boxes to assist physicians in analyzing the location of lesions in the thoracic cavity, reducing the sampling time during anesthesia, and ultimately improving the diagnosis of lung cancer staging.

2. Related Work

2.1. DEtection TRansformer (DETR)

DETR is a object detection model based on the Transformer architecture [23]. Its core idea is to utilize the attention mechanism (Multi-head Attention) to capture information from the entire image in a global context. The model initially extracts features from the image using a convolutional neural network and introduces positional encoding to preserve location information. The reduced feature map, combined with spatial position encoding, is then input into the encoder. The encoder employs a self-attention mechanism to weight different positions in the input, capturing global information. The final result of the encoder is the features encoded for N objects.

Next is the decoder, where each decoder takes two inputs: an object query and the output of the encoder, used to decode information for N objects. Each layer of the decoder calculates losses and includes learnable positional encoding. Finally, two feed-forward networks generate predicted detection boxes and categories.

Compared to other deep learning architectures, the attention mechanism can capture long-term relationships at different positions and assign different weights based on the importance of different parts of the data. Additionally, when processing images, it can globally capture information. Therefore, it is widely popular in image classification or object detection tasks.

2.2. Semi-supervised learning method

Semi-supervised learning is a machine learning approach that enhances model performance by effectively utilizing both labeled and unlabeled datasets. In the practical training process, labeled data incurs significant human and time costs, while unlabeled data is relatively easier to obtain. Semi-supervised learning can efficiently leverage unlabeled data to improve the model's generalization performance.

A common method in semi-supervised learning is label propagation. In label propagation, the model initially undergoes supervised learning using labeled data to learn how to predict labels. Subsequently, the model's predictions on unlabeled data are used as pseudo-labels. These pseudo-labels, along with the labeled data, are then employed for further training, allowing the model to glean more information about data structures and representations from the unlabeled data. Zhang's team introduced a teacher-student framework into DETR [18], incorporating different data augmentation effects for unlabeled data. The data is fed into both the student and teacher models, and the outputs of both are used to calculate the loss function, effectively utilizing unlabeled data. This approach has demonstrated significant effectiveness in semi-supervised learning on public datasets.

2.3. Optical flow method

The optical flow method utilizes the temporal variations of pixels in an image sequence and the correlation between adjacent frames to establish the correspondence between the previous and current frames. This enables the calculation of motion information for objects between consecutive frames, as depicted in Figure 2. Consequently, optical flow is crucial in applications such as motion analysis and object tracking. The underlying principle is based on the assumption of brightness constancy, meaning that the brightness in the image remains relatively constant. By analyzing the brightness changes in the image, the method computes the motion vectors for each pixel, forming an optical flow field. It has been applied in many object detection tasks and has good performance. [24][25]

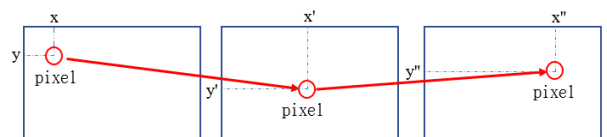


Figure 2. Optical flow method diagram.

3. Material and Methods

3.1. EBUS-TBNA Dataset

This study collected data from patients who underwent EBUS-TBNA at the Chest Department of the National Taiwan University Cancer Center Hospital between November 2019 and April 2021, totaling 151 individuals. Video data from the examinations were stored using the medical imaging recording system. The dataset consists of 1183 annotated grayscale images of lesions. For data segmentation, images taken after November 27, 2020, were designated as the test dataset, comprising 214 annotated images. Data collected before November 27, 2020, were randomly split into training and validation datasets on a per-patient basis. The training set includes 798 annotated images, and the validation set includes 171 annotated images. The study protocol was approved by the National Taiwan University Cancer Center Institutional Review Board (IRB #202105105RIND).

3.2. Experimental Procedure

The experimental workflow is illustrated in Figure 3. The study begins with data collection, where patients are divided into training, validation, and test sets. Then, the optical flow method is used to amplify the annotation data on the training set to compare the performance difference of models with and without optical flow. For model design, we reference previous research on video object detection models, initially designing a video object detection model based on DETR. Subsequently, a semi-supervised learning method is designed for further optimization. Finally, the study conducts multiple tests, including:

- (1) Comparison of test results for various models.
- (2) Test the effectiveness of optical flow method in generating pseudo labels on EBUS-TBNA images.
- (3) Testing before and after the application of semi-supervised learning methods.

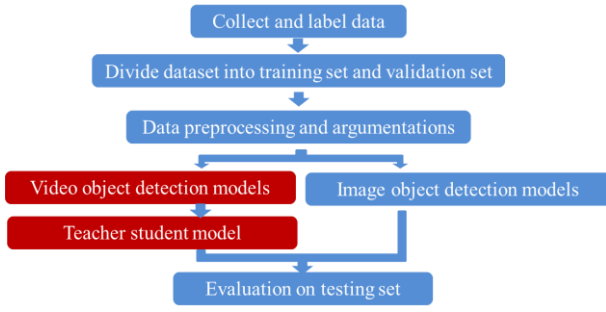


Figure 3. Experiment process

3.3. Data Preprocessing

The preprocessing pipeline is illustrated in Figure 4. To reduce the computational load, the study employs

fixed-size and positioned cropping on the original image (1920×1200) focusing on the EBUS-TBNA image, which is then resized to a suitable dimension (224×224). In EBUS-TBNA videos, the lesion's position changes over time, and each frame's lesion is related. In this study, videos were divided into small clips with a duration of five seconds, and frames were sampled at a rate of one frame per second. The physician's annotated data had a labeling frequency of two seconds per frame. For the unannotated intervals, we experimented with using optical flow and a teacher-student model to generate pseudo-labels. Subsequently, these labels were stacked to form 3D dynamic images (clips) as input. The size of each clip is $224 \times 224 \times 5$. Currently, we haven't incorporated data augmentation, but it will be added in the future and tested.

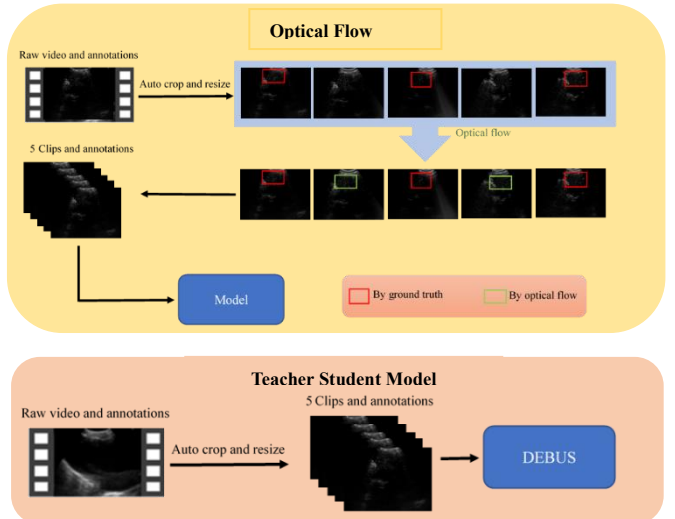


Figure 4. preprocessing flow chart

3.4. Model Overview

The model designed in this study is referred to as DEBUS, as depicted in Figure 5. DEBUS is constructed based on the architecture of DETR. It includes 3DETR, which is capable of capturing temporal information in the videos. Through the teacher-student model in semi-supervised learning, the model is further optimized using the unlabeled dataset. The following sections will provide an introduction to these two components.

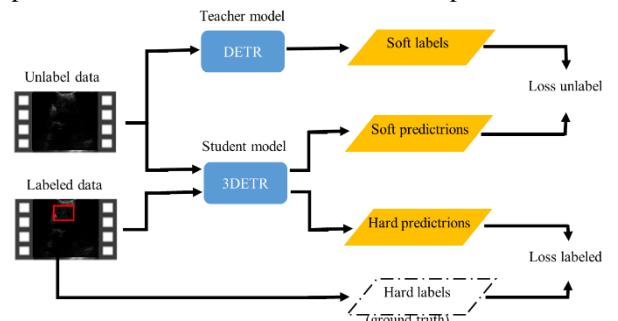


Figure 5. Overview of DEBUS

3.4.1. 3DETR (Video Object Detection)

3DETR, as illustrated in Figure 6., is a model designed in this study to capture temporal information in videos. We utilize a 2D CNN to extract features from each frame of the image. The extracted features from each frame are then separately input into the encoder of DETR for encoding. The encoding results of each frame are then fed into the decoder, where an attention mechanism is employed with the previous frame for attention calculation. This process is repeated until the last frame, effectively preserving temporal information. In this case, the number of layers in the encoder follows the design of DETR, with a total of six layers. The decoder is adapted to three layers, and both the encoder and decoder share weights. In the future, we aim to tailor this architecture to the characteristics of EBUS-TBNA data. Given the substantial variations in ultrasound videos due to probe movement and shaking during EBUS-TBNA surgery, we plan to incorporate selective attention mechanisms in the propagation of relevant frames. This ensures that only helpful information is propagated to assist the prediction of the current frame. Additionally, considering the typical duration of grayscale video sequences in EBUS-TBNA (mostly around 3 to 7 seconds), we design the model to take five frames as input in a single pass. Furthermore, to verify the utility of temporal information in EBUS-TBNA, we plan to conduct separate tests using a conventional image-based object detection model for comparison.

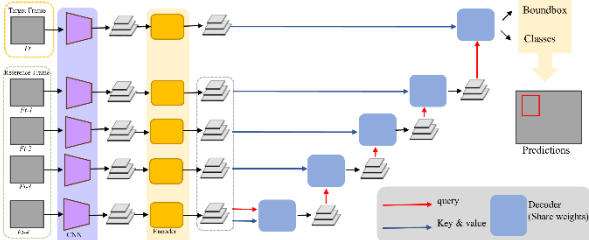


Figure 6. 3DETR model diagram

3.4.2. Semi-supervised (teacher student model)

Through our experiments, we have validated the effectiveness of video-based object detection models on EBUS-TBNA data. However, these models still struggle to effectively utilize other unlabeled data. Moreover, the requirement for continuous annotated data as input poses additional challenges in annotation. We believe that if both the teacher and student models are based on video-based object detection models, the computational resources required for training would be too extensive. Therefore, we propose using an image-based object detection model as the teacher model, not only to reduce computational resources but also to introduce noise that may appear in EBUS-TBNA data during the input of the teacher-student model. This allows the student model to

develop noise-resistant capabilities. In the subsequent loss update, we use a Gaussian Mixture Model (GMM) to filter pseudo-labels on the teacher model. Consequently, this study further applies the teacher-student model to leverage the remaining unlabeled data.

As shown in Figure 5, we use the pre-trained original DETR on the EBUS-TBNA dataset as the teacher model. It generates soft labels on the unlabeled data and calculates the loss (Loss unlabeled) based on the soft predictions of 3DETR. This process aims to enhance the model's generalization on the EBUS-TBNA dataset. The loss function is expressed as follows:

$$L_{unlabel} = (1 - \overline{IOU}) \cdot \max(score) \quad (1)$$

$$IOU = \frac{A \cap B}{A \cup B} \quad (2)$$

Here, A represents the predicted boxes within the soft labels generated by DETR, and B represents the predicted boxes within the soft predictions generated by 3DETR. We calculate the Intersection over Union (IOU) using this information, take the average, and multiply it with the confidence score of the maximum value among all predicted boxes. We believe that, compared to other loss functions, IOU better represents the accuracy of box positions, and the score is determined by DETR's confidence level, serving as the soft label.

Since it has been established through testing that the video-based object detection model performs better, this study will only conduct ablation tests on the video-based object detection model to verify the value of utilizing unlabeled data in EBUS-TBNA.

3.5. Equipment

This study utilized a server with ASUS Z790-A GAMING WIFI 6E, powered by Intel I9-13900K, and equipped with MSI RTX 4090 GAMING X TRIO 24G.

4. Result

4.1. Evaluation Methods

For all deep learning architectures, this study will use mAP (mean Average Precision) calculation as the metric to evaluate the model performance. The mAP calculation involves sorting the predicted results based on confidence scores. Different thresholds are applied to examine the predicted results. If a prediction matches the ground truth label, it is considered a true positive (TP), otherwise, it is a false positive (FP). False negatives (FN) represent the number of ground truth labels not detected. Precision is calculated as $TP/(TP+FP)$, Recall as $TP/(TP+FN)$. The Precision-Recall curve is plotted, and

the area under the curve is calculated as AP (Average Precision). mAP is the average AP across different classes. Since our task involves detecting lesions, AP is equivalent to mAP.

As there is currently no publicly available EBUS-TBNA dataset, this research relies on data provided by the National Taiwan University Cancer Center for testing and evaluation.

4.2. Implement detail

The hyperparameters used in training DEBUS in this study include an initial learning rate of 1e-4, the optimizer is Adam with Weight Decay Regularization (AdamW), the classification loss is Cross-entropy Loss, and the bounding box loss is a combination of L1 Loss and GIoU Loss. The parameters are updated every 16 data points. The total training epoch for DEBUS is 300, with a learning rate decay to 0.1 every 50 epochs.

4.3. Comparison of different models

This section aims to compare 3DETR with other image object detection models. Table 1 shows the results of different models on the test set, where YOLOX and Faster-RCNN are image object detection models compared in this section, and 3DETR is the video object detection model proposed in this study. From the results, it can be observed that the proposed model in this study outperforms other 2D models in terms of bounding box accuracy, indicating that the 3DETR architecture proposed in this study effectively captures temporal features and utilizes these features to enhance the quality of predictions.

Table 1. Comparison of different models

Model	mAP	mAP ₅₀	mAP ₇₅
YOLOX[26]	36	82.7	24.9
Faster-RCNN[27]	36.1	80.6	26.4
DETR[23]	38.9	83.4	25.7
3DETR(Ours)	49	94.4	34.5

4.4. Comparison of amplified annotations with and without optical flow method

This section aims to discuss the performance of optical flow in generating pseudo-labels. As shown in Table 4-2, applying optical flow data augmentation on most models leads to a decrease in mAP. We attribute this to the fact that the data generated by optical flow is not manually annotated by physicians, introducing noise. Additionally, in ultrasound images, each frame is a result of ultrasound echoes, and, as a result, the constant brightness assumption of optical flow is invalid. As the

position and angle of ultrasound vary, the brightness of the lesion differs. Lesion position in the image is also determined by the relative brightness of the same image. This result indicates that traditional optical flow methods are not suitable for the EBUS-TBNA dataset.

Table 2. Optical flow data set in different model
(†: with optical flow)

Model	mAP	mAP ₅₀	mAP ₇₅
YOLOX[26]	36	82.7	24.9
YOLOX†[26]	35.6	79.4	25.6
Faster-RCNN[27]	36.1	80.6	26.4
Faster-RCNN†[27]	32.8	71.5	25.1
DETR[23]	38.9	83.4	25.7
DETR†[23]	35.3	82.1	22.4
3DETR(Ours)	41.6	86.5	31.6
3DETR†(Ours)	37.6	82.6	28.5

4.5. Comparison of semi-supervised learning applications in video object detection models

This section aims to discuss the performance of semi-supervised learning applied to video object detection models for medical imaging. Table 4-3 demonstrates that models with semi-supervised learning achieve higher mAP values. On the test set, there is a slight improvement in mAP (+0.3), and a significant improvement in mAP₇₅ (+5.5). This validates the effectiveness of semi-supervised learning for the challenging EBUS-TBNA dataset, where labeling is difficult. Through this approach, the model can learn spatial features from unlabeled EBUS-TBNA data, enhancing its generalization and accuracy on EBUS-TBNA. Compared to traditional optical flow methods, using a teacher-student model to provide pseudo-labels in EBUS-TBNA is feasible and practical.

Table 3. Video object detection model adds semi-supervised learning results (†: with optical flow)

Model	mAP	mAP ₅₀	mAP ₇₅
3DETR(Ours)	41.6	86.5	31.6
DEBUS(Ours)	41.9	84.5	37.1

5. Conclusion

In the current study, the proposed DEBUS model achieves a prediction box accuracy of 41.6 mAP and 37.1 mAP₇₅ on the test set of EBUS-TBNA images. The 3DETR component in DEBUS, leveraging its excellent ability to extract temporal features, outperforms other image object detection model architectures. Additionally, the effective utilization of unlabeled data through semi-supervised learning further enhances DEBUS's performance.

There is room for improvement in the proposed model. In the future, incorporating filtering mechanisms in 3DETR to remove frames with significant differences before and after could increase the model's robustness. Furthermore, introducing mechanisms in semi-supervised learning to enhance the model's performance and incorporating additional data augmentation in data preprocessing could be explored.

However, there are limitations to this study. The dataset is sourced from a single hospital, and variations in equipment between hospitals may result in different feature distributions. The model may not generalize well to datasets from other hospitals. Future work could involve obtaining more diverse training data to enable the model to learn a broader range of lesion features, thereby improving its performance, robustness, and generalizability.

6. Reference

[1] A. Jemal, R. Siegel, E. Ward, Y. Hao, J. Xu, and M. Thun, "Cancer statistics," *Ca Cancer J Clin*, vol. 59, no. 4, 2009.

[2] K. Yasufuku and T. Fujisawa, "Staging and diagnosis of non-small cell lung cancer: invasive modalities," *Respirology*, vol. 12, no. 2, pp. 173-183, 2007.

[3] K. Yasufuku et al., "Real-time endobronchial ultrasound-guided transbronchial needle aspiration of mediastinal and hilar lymph nodes," *Chest*, vol. 126, no. 1, pp. 122-128, 2004.

[4] T. Nakajima et al., "The role of EBUS-TBNA for the diagnosis of sarcoidosis—comparisons with other bronchoscopic diagnostic modalities," *Respiratory medicine*, vol. 103, no. 12, pp. 1796-1800, 2009.

[5] N. Navani et al., "Lung cancer diagnosis and staging with endobronchial ultrasound-guided transbronchial needle aspiration compared with conventional approaches: an open-label, pragmatic, randomised controlled trial," *The Lancet Respiratory Medicine*, vol. 3, no. 4, pp. 282-289, 2015.

[6] C. K. Lin, C. L. Lai, L. Y. Chang, Y. F. Wen, and C. C. Ho, "Learning curve and advantages of endobronchial ultrasound-guided transbronchial needle aspiration as a first-line diagnostic and staging procedure," *Thoracic cancer*, vol. 9, no. 1, pp. 75-82, 2018.

[7] Fujiwara, T., Yasufuku, K., Nakajima, T., Chiyo, M., Yoshida, S., Suzuki, M., Shibuya, K., Hiroshima, K., Nakatani, Y., & Yoshino, I. (2010). The utility of sonographic features during endobronchial ultrasound-guided transbronchial needle aspiration for lymph node staging in patients with lung cancer: a standard endobronchial ultrasound image classification system. *Chest*, 138(3), 641–647.

[8] Nakajima, T., Anayama, T., Shingyoji, M., Kimura, H., Yoshino, I., & Yasufuku, K. (2012).

Vascular image patterns of lymph nodes for the prediction of metastatic disease during EBUS-TBNA for mediastinal staging of lung cancer. *Journal of thoracic oncology : official publication of the International Association for the Study of Lung Cancer*, 7(6), 1009–1014.

[9] Izumo, T., Sasada, S., Chavez, C., Matsumoto, Y., & Tsuchida, T. (2014). Endobronchial ultrasound elastography in the diagnosis of mediastinal and hilar lymph nodes. *Japanese journal of clinical oncology*, 44(10), 956–962. <https://doi.org/10.1093/jjco/hyu105>

[10] Xianhua Zeng, Li Wen, Banggui Liu, Xiaojun Qi, Deep learning for ultrasound image caption generation based on object detection, *Neurocomputing*, Volume 392, 2020.

[11] Bose, A., Nguyen, T., Du, H., AlZoubi, A. (2022). Faster RCNN Hyperparameter Selection for Breast Lesion Detection in 2D Ultrasound Images. In: Jansen, T., Jensen, R., Mac Parthaláin, N., Lin, CM. (eds) *Advances in Computational Intelligence Systems*. UKCI 2021. *Advances in Intelligent Systems and Computing*, vol 1409. Springer, Cham.

[12] Snider, E.J.; Hernandez-Torres, S.I.; Avital, G.; Boice, E.N. Evaluation of an Object Detection Algorithm for Shrapnel and Development of a Triage Tool to Determine Injury Severity. *J. Imaging* 2022, 8, 252. <https://doi.org/10.3390/jimaging8090252>

[13] CAO, Guimei, et al. Feature-fused SSD: Fast detection for small objects. In: Ninth international conference on graphic and image processing (ICGIP 2017). SPIE, 2018. p. 381-388.

[14] Y. Tang, H. Chen, L. Qian, S. Ge, M. Zhang and R. Zheng, "Detection of Spine Curve and Vertebral Level on Ultrasound Images Using DETR," 2022 IEEE International Ultrasonics Symposium (IUS), 2022, pp. 1-4, doi: 10.1109/IUS54386.2022.9958621.

[15] M. Fujitake and A. Sugimoto, "Video Sparse Transformer With Attention-Guided Memory for Video Object Detection," in *IEEE Access*, vol. 10, pp. 65886-65900, 2022, doi: 10.1109/ACCESS.2022.3184031.

[16] Zhou, Q., Li, X., He, L., Yang, Y., Cheng, G., Tong, Y., ... & Tao, D. (2022). TransVOD: end-to-end video object detection with spatial-temporal transformers. *IEEE Transactions on Pattern Analysis and Machine Intelligence*.

[17] Wang, H., Tang, J., Liu, X., Guan, S., Xie, R., & Song, L. (2022, October). Ptseformer: Progressive temporal-spatial enhanced transformer towards video object detection. In *European Conference on Computer Vision* (pp. 732-747). Cham: Springer Nature Switzerland.

[18] Zhang, J., Lin, X., Zhang, W., Wang, K., Tan, X., Han, J., ... & Li, G. (2023). Semi-DETR: Semi-Supervised Object Detection With Detection Transformers. In *Proceedings of the IEEE/CVF Conference on Computer Vision and Pattern Recognition* (pp. 23809-23818).

[19] Wang, Xinjiang, et al. "Consistent Targets

Provide Better Supervision in Semi-supervised Object Detection." arXiv preprint arXiv:2209.01589 (2022).

[20] Liu, Y. C., Ma, C. Y., & Kira, Z. (2022). Unbiased teacher v2: Semi-supervised object detection for anchor-free and anchor-based detectors. In Proceedings of the IEEE/CVF Conference on Computer Vision and Pattern Recognition (pp. 9819-9828).

[21] Zhu, X., Su, W., Lu, L., Li, B., Wang, X., & Dai, J. (2020). Deformable detr: Deformable transformers for end-to-end object detection. arXiv preprint arXiv:2010.04159.

[22] Dai, X., Chen, Y., Yang, J., Zhang, P., Yuan, L., & Zhang, L. (2021). Dynamic detr: End-to-end object detection with dynamic attention. In Proceedings of the IEEE/CVF International Conference on Computer Vision (pp. 2988-2997).

[23] Carion, N., Massa, F., Synnaeve, G., Usunier, N., Kirillov, A., & Zagoruyko, S. (2020, August). End-to-end object detection with transformers. In European conference on computer vision (pp. 213-229). Cham: Springer International Publishing.

[24] Huang, J., Zou, W., Zhu, J., & Zhu, Z. (2018). Optical flow based real-time moving object detection in unconstrained scenes. arXiv preprint arXiv:1807.04890.

[25] Fan, L., Zhang, T., & Du, W. (2021). Optical-flow-based framework to boost video object detection performance with object enhancement. Expert Systems with Applications, 170, 114544.

[26] Ge, Z., Liu, S., Wang, F., Li, Z., & Sun, J. (2021). Yolox: Exceeding yolo series in 2021. arXiv preprint arXiv:2107.08430.

[27] Ren, S., He, K., Girshick, R., & Sun, J. (2015). Faster r-cnn: Towards real-time object detection with region proposal networks. Advances in neural information processing systems, 28.